J Biol Inorg Chem (2009) 14:1253–1263
DOI 10.1007/s00775-009-0569-6

ORIGINAL PAPER

Biomimetic oxidative treatment of spruce wood studied by pyrolysis–molecular beam mass spectrometry coupled with multivariate analysis and ^{13}C-labeled tetramethylammonium hydroxide thermochemolysis: implications for fungal degradation of wood

Valdeir Arantes · Yuhui Qian · Stephen S. Kelley · Adriane M. F. Milagres · Timothy R. Filley · Jody Jellison · Barry Goodell

Received: 18 March 2009 / Accepted: 8 July 2009 / Published online: 21 July 2009

Abstract In this work, pyrolysis–molecular beam mass spectrometry analysis coupled with principal components analysis and ^{13}C-labeled tetramethylammonium hydroxide thermochemolysis were used to study lignin oxidation, depolymerization, and demethylation of spruce wood treated by biomimetic oxidative systems. Neat Fenton and chelator-mediated Fenton reaction (CMFR) systems as well as cellulosic enzyme treatments were used to mimic the nonenzymatic process involved in wood brown-rot biodegradation. The results suggest that compared with enzymatic processes, Fenton-based treatment more readily opens the structure of the lignocellulosic matrix, freeing cellulose fibrils from the matrix. The results demonstrate that, under the current treatment conditions, Fenton and CMFR treatment cause limited demethoxylation of lignin in the insoluble wood residue. However, analysis of a water-extractable fraction revealed considerable soluble lignin residue structures that had undergone side chain oxidation as well as demethoxylation upon CMFR treatment. This research has implications for our understanding of nonenzymatic degradation of wood and the diffusion of CMFR agents in the wood cell wall during fungal degradation processes.

Keywords Pyrolysis–molecular beam mass spectrometry · Principal components analysis · ^{13}C-tetramethylammonium hydroxide · Lignin · Demethoxylation

V. Arantes
Department of Wood Science,
Faculty of Forestry,
University of British Columbia,
2424 Main Mall,
Vancouver, BC V6T 1Z4,
Canada
e-mail: varantes@forestry.ubc.ca

Y. Qian · B. Goodell (✉)
Wood Science and Technology, SFR,
University of Maine,
5755 Nutting Hall,
Orono, ME 04469-5755,
USA
e-mail: goodell@umit.maine.edu

S. S. Kelley
Department of Wood and Paper Science,
North Carolina State University,
Raleigh, NC,
USA

A. M. F. Milagres
Department of Biotechnology,
Escola de Engenharia de Lorena,
University of São Paulo,
Lorena, SP, Brazil

T. R. Filley
Department of Earth and Atmospheric Sciences,
Purdue University,
West Lafayette, IN, USA

J. Jellison
Department of Biological Sciences,
University of Maine,
Orono, ME,
USA

Introduction

The biodegradation of woody materials, the most abundant biomass on earth, is one of the most important processes in terrestrial forested ecosystems. Wood-decay fungi are some of the few organisms that can utilize or degrade nearly all biochemical forms of carbon in woody tissue facilitating the return of CO_2 to the atmosphere [1]. Wood is the most abundant plant-derived biomass on earth and it consists primarily of cellulose, hemicellulose, and lignin. Brown-rot basidiomycete fungi preferentially attack coniferous woods, and brown rot is also the most common and most destructive type of decay in structural wood products in the northern hemisphere [2].

Brown-rot fungi do not cause appreciable loss of lignin during wood degradation [3, 4], but instead primarily attack the holocellulose component of wood, eventually leaving an amorphous, brown, and crumbly residue of modified lignin. The methoxyl carbons of lignin are often removed, generating a demethoxylated aromatic product with high degree of *ortho*-dihydroxy substitution [5–10]. Although the oxidation of aliphatic side chains occurs, lignin is further altered and depolymerized to a very limited extent by brown-rot fungi [5].

In early stages of brown-rot decay, extensive depolymerization of the cellulose within the wood cell wall occurs at very low weight loss, which causes the wood to rapidly lose strength in comparison with the rate of wood metabolism. Cowling [3] first recognized that conventional enzymes were too large to penetrate into the intact wood cell wall. It is now well established that the initial stages of decay involve the nonenzymatic action of highly destructive hydroxyl radicals produced by extracellular Fenton chemistry [11–13]. In addition, it has been shown that phenolic compounds such as 2,5-dimethoxy-1,4-bezoquinone and 4,5-dimethoxy-1,2-bezoquinone, produced by the fungi, and also biomimetic fungal phenolic compounds [11, 13–18] act as ferric iron chelators and sources of electrons for iron reduction, and thus promote the Fenton reaction. However, the exact mechanism of nonenzymatic brown-rot decay by various fungi is still being resolved [12, 19].

Although the rapid degradation of holocellulose components during fungal degradation is well established, it has been demonstrated that a close relationship between lignin demethylation and polysaccharide loss during wood biodegradation by brown-rot fungi exists [20]. This suggests that demethylation may play a mechanistic role in polysaccharide loss, possibly by assisting in Fenton reactions [20, 21]. It has been widely assumed that lignin demethoxylation during wood degradation by brown-rot fungi occurs via attack of reactive oxygen species generated through the action of Fenton chemistry [22]. Studies have shown that hydroxyl radicals can lead to hydroxylation and/or demethoxylation of lignin model compounds [17, 23–26]. However, to date there has been no practical demonstration that a chelator-mediated Fenton reaction (CMFR) system (Fe^{3+}, H_2O_2, and an Fe^{3+}-reducing agent) can cause lignin demethoxylation in wood.

To understand the action of the CMFR system better, we used pyrolysis–molecular beam mass spectrometry (py-MBMS) techniques in conjunction with multivariate regression and principal components analysis to monitor the chemical composition of wood to follow the subtle chemical structural difference in wood as it undergoes CMFR treatments. The ^{13}C-tetramethylammonium hydroxide (TMAH) thermochemolysis technique was also applied to characterize chemical modifications of lignin in wood subjected to CMFR treatments [8, 22].

Materials and methods

Chemicals and ground spruce wood treatment

$FeSO_4$, $FeCl_3$, $MnCl_2$, $CuCl_2$, 2,3-dihydroxybenzoic acid, hydrogen peroxide, cellulase from *Trichoderma reesei*, and hemicellulase from *Aspergillus niger* were purchased from Sigma Chemical (St. Louis, MO, USA). Deionized water was used in all chemical and sample preparations. Red spruce (*Picea rubens*) sapwood was ground to 40 mesh for all the experiments.

To prepare samples for the py-MBMS study, milled wood was treated using one of the reaction conditions outlined in Table 1. For each condition, the treatment was performed in five replicates. Unless otherwise indicated, all treatments were carried out in 40-ml glass tubes at 30 °C with constant gentle shaking. Ground wood (0.5 g) was first placed in each tube containing pH 4.5 acetate buffer. Measured amounts of chemicals/enzymes were then added to the suspension. The final buffer strength was 50 mM, and all chemical/enzyme doses were as listed in Table 1 based on a final reaction volume of 20 ml. After 60 h, the reaction mixture was centrifuged to remove the supernatant. The remaining wood residue was then dried at room temperature in the dark for further analysis.

Red spruce wood samples (50 mg each) were prepared using the reagents specified in Table 2, at 30 °C with constant gentle shaking for ^{13}C-TMAH thermochemolysis. After 30 h, the reaction mixture was centrifuged to separate the supernatant, which was carefully collected and freeze-dried, and the residue was dried in the absence of light. A control and a reference sample were used, the former consisting of ground wood and buffer, and the latter containing Fe^{3+} as a substitute for Fe^{2+} (as $FeSO_4$) and omitting 2,3-dihydroxybenzoic acid. Before analysis by

Table 1 Chemical/enzyme loading in the samples prepared for pyrolysis–molecular beam mass spectrometry analysis

Group	$FeCl_3$ (mM)	$MnCl_2$ (mM)	$CuCl_2$ (mM)	DHBA (mM)	H_2O_2 (mM)	Cellulase (units)	Hemicellulase (units)
1	–	–	–	–	–	–	–
2	–	–	–	–	–	100	100
3	0.5	–	–	0.25	1	–	–
4	–	0.5	–	0.25	1	–	–
5	–	–	0.5	0.25	1	–	–
6	0.5	–	–	0.25	1	–	–
7	0.5	–	–	0.25	1	–	–
8	0.5	–	–	0.25	1	100	100
9	–	0.5	–	0.25	1	100	100
10	–	–	0.5	0.25	1	100	100
11	0.5	–	–	0.25	1	100	100
12	–	0.5	–	0.25	1	100	100
13	–	–	0.5	0.25	1	100	100
14	0.5	–	–	0.25	1	100	100
15	–	0.5	–	0.25	1	100	100
16	–	–	0.5	0.25	1	100	100

For condition 6, chemicals were drained and replaced with iron only every 12 h. For condition 7, chemicals were drained and then replaced with fresh mediated-Fenton chemicals every 12 h. For conditions 8–10, enzymes were added first, and the rest of the chemicals were added 2 h later. For conditions 11–13, Fenton chemicals were added first, and then enzymes were added 8 h later. For conditions 14 to 16, the treatment was the same as for conditions 11–13, except that the wood samples were washed three times before the addition of enzymes. For each condition, five replicates were prepared and analyzed

Table 2 Chemical loading in the samples prepared for ^{13}C-tetramethylammonium hydroxide thermochemolysis

	$FeSO_4$ (mM)	$FeCl_3$ (mM)	DHBA (mM)	H_2O_2 (mM)	pH 4.5 buffer (mM)
Control	–	–	–	–	50
Fenton	0.5	–	–	1	50
CMFR	–	0.5	0.25	1	50

CMFR chelator-mediated Fenton reaction

^{13}C-TMAH thermochemolysis, the dried samples were milled using a laboratory ball mill (no. 40 mesh).

Pyrolysis–molecular beam mass spectrometry

The py-MBMS analyses were carried out using a pyrolysis furnace coupled to a molecular beam mass spectrometer [27–29].

Approximately 20–30 mg of ground sample material was loaded into a pyrolysis furnace preheated to 550 °C. The molecular fragments were swept into the molecular beam mass spectrometer with a stream of helium gas. The gas stream was expanded through three vacuum chambers where most intermolecular collisions were quenched by the near adiabatic expansion of gases. A low-energy electron beam (approximately 23 eV) was used to ionize the molecular beam to yield a positive ion mass spectrum.

The py-MBMS spectra were collected in duplicate for each of the five samples produced for each experimental condition. These two spectra were averaged to create a single spectrum for the samples, and all "averaged" spectra were included in the principal components analysis (PCA).

Principal components analysis

Details of the multivariate analysis have been described elsewhere [30, 31]. The mass spectra were normalized to the total ion current, and fragments (*m*/*z* value) between 60 and 310 were used in the multivariate analysis to provide 250 data points for each sample and no further preprocessing was done before conducting a standard PCA with the Unscrambler® (CAMO, Corvallis, OR, USA) software program. To aid in the interpretation of the results, the PCA technique was used to reduce data complexity, and to visualize the relationship between wood chemical components in the samples treated under the specified conditions.

^{13}C-TMAH thermochemolysis

^{13}C-labeled TMAH was synthesized as described in Filley et al. [32]. ^{13}C-TMAH thermochemolysis was performed in-line using a Shimadzu Pyr-4a pyrolysis unit. Samples were weighed (typically 100–150 μg) into platinum buckets, which were precharged with an eicosane internal

standard. After sample addition, 3 µl of a 25 wt% solution of ^{13}C-TMAH in water was added. The buckets were then placed in a sample holder affixed to the top of the Pyr-4a unit for 15 min, maintaining the bucket at room temperature under a helium gas stream. The sample bucket was then delivered into the hot zone of the unit at 350 °C. The injector base of the Pyr-4a unit was maintained at 320 °C with a flow split of 20:1.

Chromatography and mass-spectral analysis of the products from the ^{13}C-TMAH thermochemolyisis was performed using a GC17A gas chromatograph interfaced to a QP5050A quadrupole mass spectrometer collecting in the mass range *m/z* 40–550. Chromatographic separation was performed on a fused-silica column (Restek RTx-5, 30 m, 0.25-mm inner diameter, film thickness 0.25 µm). The oven was temperature programmed from 60 °C (1-min hold) to 300 °C at 7 °C/min and maintained at that temperature for 15 min.

Determination of aromatic hydroxyl content

Each of the eight permethylated guaiacyl compounds in Fig. 7 was investigated for their original aromatic hydroxyl content by analysis of the number of ^{13}C methyl groups added during thermochemolysis methylation, using the mass-spectral methods outlined by Filley et al. [32], and the results for treated wood were expressed as the percentage of demethoxylation in relation to untreated wood.

Results and discussion

PCA of the py-MBMS difference spectra

The py-MBMS spectra of the samples treated under the specified conditions (Table 1) showed that most of the major fragment peaks could be assigned to wood carbohydrate and lignin components (data not shown). For example, masses at *m/z* of 60, 73, 85, 98, 114, and 126 are typically associated with cellulose/hemicellulose degradation products, and peaks at *m/z* of 124, 137, 150, 154, 167, 180, 194, 210, and 272 are all associated with different lignin fragments [18, 19, 30, 33, 34].

The PCA results of the py-MBMS analysis are shown in Fig. 1. Figure 1a shows all samples in a PCA score plot of principal componnet 1 (PC1) versus principal component 2 (PC2), whereas Fig. 1b shows the PCA loading of PC1 and PC2. The plot of PC1 versus PC2 contains 62% of the py-MBMS spectral variation, 52% for PC1 and 10% for PC2. It is clear that samples 7, 3, 11, and 14 formed distinct groups (outlined as oval groups in Fig. 1a) that are strongly positive along PC1. The sample 7 group is also distinctly negative along PC2. As specified in the treatment

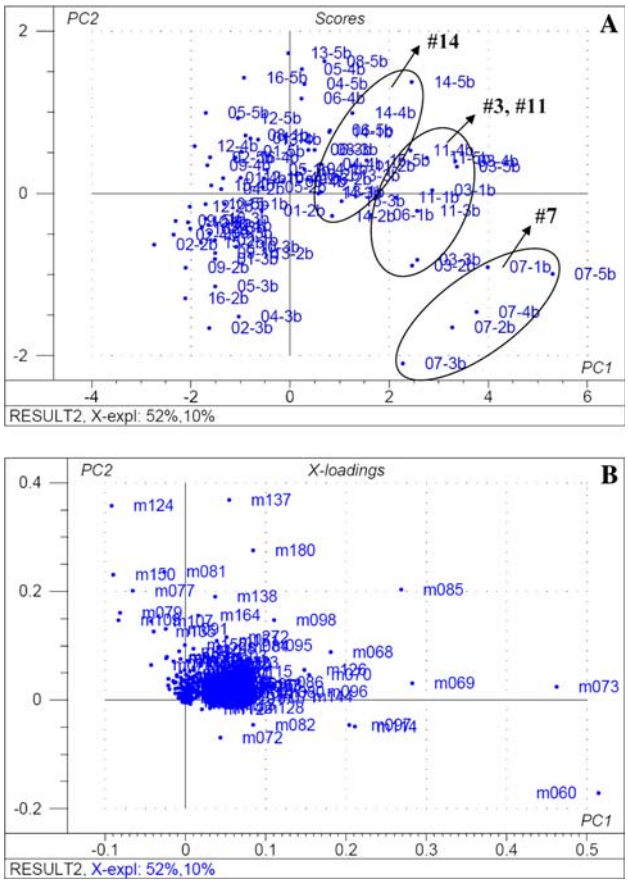

Fig. 1 **a** The principal components analysis (PCA) score plot of the pyrolysis–molecular beam mass spectrometry (py-MBMS) spectra of all the samples (1–16), which reveals three distinct clusters (indicated by the *ovals*) separated along principal component 1 (*PC1*) or principal component 2 (*PC2*). **b** The loadings for PC1 and PC2

conditions listed in Table 1, all samples contained in these groupings were subjected to prolonged Fenton treatment: sample 3 was treated with iron-based Fenton chemicals for 60 h; sample 7 was treated with fresh Fenton chemicals every 12 h; and samples 11 and 14 were subjected to Fenton treatment for at least 8 h. Other samples did not form distinguishable groups along PC1 or PC2 in this plot. Harsh Fenton treatment would be expected to produce significant changes in the chemical composition of wood samples. Upon close inspection of the PCA loading (Fig. 1b), it was found that the chemical features distinguishing these groups from the rest of the samples were related to a high percentage of carbohydrate fragments. The loadings show that PC1 is driven by fragments assigned to C_5 carbohydrates (*m/z* 73, 85, 96, and 114), C_6 carbohydrates (*m/z* 98 and 126), other carbohydrate fragments (*m/z* 60 and 144), and furan structures, probably derived from altered carbohydrates (*m/z* 68 and 69). PC2 loadings also indicate that the separation along this component is primarily due to methoxylated lignin related

fragments, e.g., *m/z* 124 (guaiacol), 137 and 180 (coniferyl alcohol, CA), 138 (methylguaiacol), 150 (vinylguaiacol), and 164 (propenyl guaiacol).

Figure 1b shows that the cellulose/hemicellulose fragments and lignin fragments are directly correlated in the loadings for PC1 and PC2, respectively. This suggests that group 7 samples, the CMFR samples without enzyme treatment, contained more cellulose/hemicellulose sugars and less methoxylated lignin than the rest of the samples. The overall results suggest that iron-based Fenton treatments generally produce samples with relatively more carbohydrate. This result, however, is in direct contrast with our knowledge of Fenton chemistry and previous literature describing the attack of lignocellulose materials by hydroxyl radicals [11, 21]. Fenton chemistry and reactive oxygen species are believed to degrade cellulose/hemicellulose more readily than lignin because the former fraction is more readily oxidized. Lignin depolymerization does readily occur during Fenton action, even under acidic conditions; however, the lignin monomers rapidly repolymerize [33–35]. This permits repolymerized modified lignin to be formed. It was observed in our current work that particulate materials were produced in all samples; however, the Fenton treatments generated much more fine particulate material than the other treatments. To evaluate this further, after the final centrifugation step, the supernatant was carefully removed. For all samples, we observed that when residual fines were present, they were deposited on the surface layer of the wood residue pellet. With the Fenton-treated samples, when collecting samples for py-MBMS analysis, we observed that the sample consisted primarily of fine particulates, whereas larger particles were primarily present in other samples. This suggested that Fenton treatments were effectively able to degrade the lignocellulosic matrix, solubilizing more of the lignin fraction but also producing more fines that contained a higher proportion of cellulose component with less lignin. To confirm this, we analyzed the supernatant from Fenton-treated and non-Fenton-treated samples by ^{13}C-TMAH thermochemolysis as detailed below (see also "Lignin demethoxylation").

When all the samples are included in a single analysis (Fig. 1; samples 1–16 from Table 1) differences are minimized and difficult to visualize. Therefore, in subsequent figures, the samples have been divided into subgroups to study the effect of more specific treatment conditions on the changes of wood chemical composition.

Figure 2a compares the control samples (1) with samples treated with the iron-based Fenton system (3) and the systems in which iron was replaced by manganese (4) or copper (5) salts. It is clear that data set 3 is grouped together and separated from the rest of the sample sets along PC1 (53% of the variations), but that all of the samples are indistinguishable along PC2. There are no

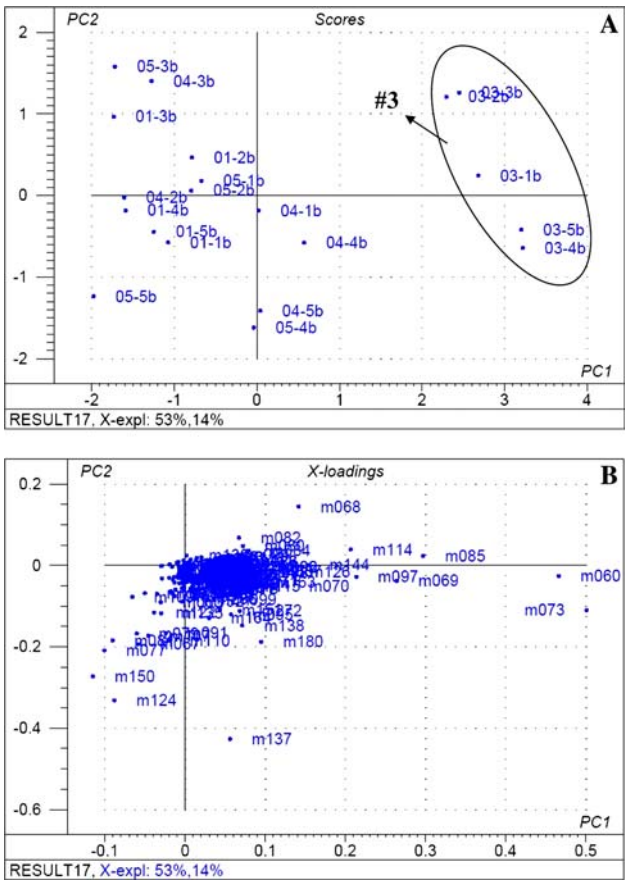

Fig. 2 **a** The PCA score plot of the py-MBMS spectra of samples 1, 3, 4, and 5. **b** The loadings for PC1 and PC2

differences between the control samples and the samples treated with manganese or the copper system. This supports findings of Contreras et al. [19], who found that the copper–catechol redox potential was inadequate to promote oxidation of either lignin or cellulose. The loadings for PC1 (Fig. 2b) reveal that the separation of sample 3 is likely due to its high carbohydrate content (*m/z* 60, 69, 73, 85, 114, and 144) and the solubilization of aromatic compounds as previously discussed.

To compare the effect of the Fenton treatment versus the effect of CMFR treatment, PCA was conducted (Fig. 3) on samples treated with:

1. The neat Fenton system (sample 3)
2. The Fenton system initially, followed by the addition of iron (sample 6)
3. Fresh Fenton chemicals repeatedly (sample 7).

Figure 3 demonstrates clear grouping and separation of the data along PC1 due primarily to the differences in carbohydrate fragment content (*m/z* 60, 69, 73, 97, and 114). Repeated Fenton treatment led to the generation of more fine particulate matter in the sample and the data show that this material contained more carbohydrate than other samples.

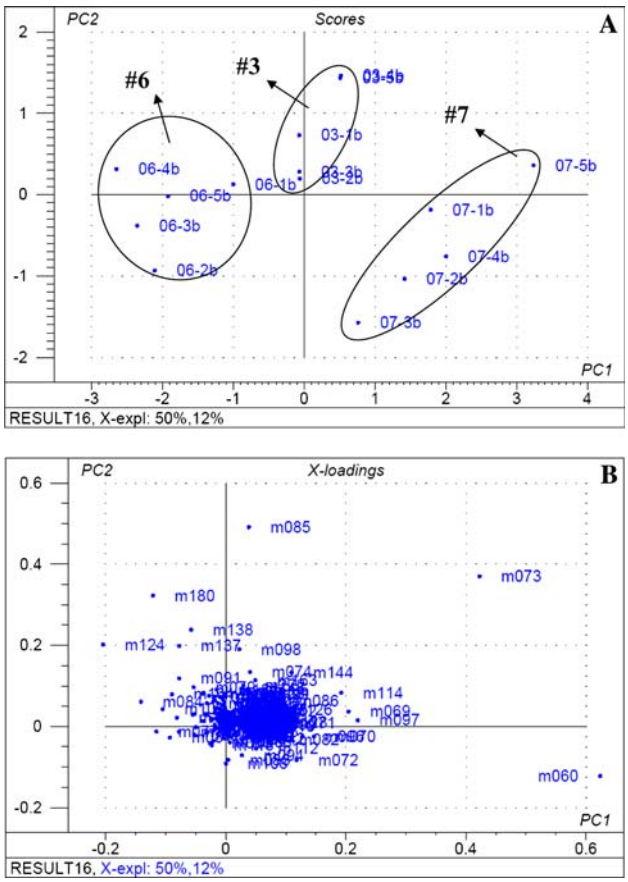

Fig. 3 **a** The PCA score plot of the py-MBMS spectra of samples 3, 6, and 7. **b** The loadings for PC1 and PC2

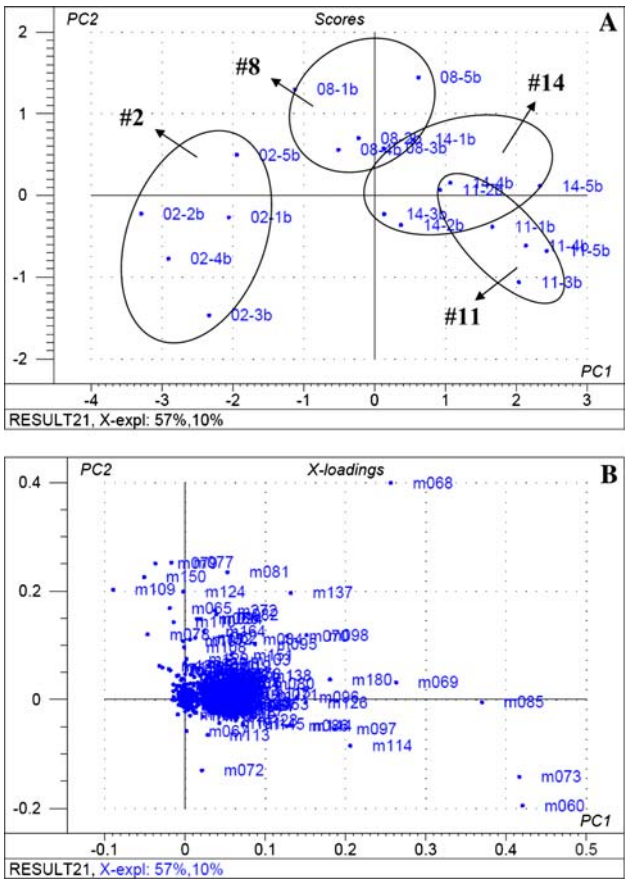

Fig. 4 **a** PCA score plot of the py-MBMS spectra of samples 2, 8, 11, and 14. **b** The loadings for PC1 and PC2

To simulate, and evaluate, the different ways in which the brown-rot process may occur, an enzymatic treatment was carried out either before or after the Fenton treatment. Figure 4 shows the PCA result of four samples: enzymes alone (sample 2), enzymatic treatment followed by Fenton reaction (sample 8), Fenton treatment followed by enzyme addition (sample 11), and Fenton treatment followed by washing prior to enzymatic treatment (sample 14).

In Fig. 4 there is a clear separation between sample 2 and other samples along PC1. Sample 2 was treated with the enzymes only and is more negative along PC1, indicating that sample 2 contains much less carbohydrate (*m*/*z* 60, 68, 69, 73, 85, 97, and 114). Both sample 11 and sample 14 remain more positive along PC1, but there is no substantial difference between these two samples. The samples treated with enzymes followed by Fenton chemicals (8) are grouped in the middle. As discussed previously, the separation of Fenton-treated samples was probably due to the high carbohydrate content of the fines in the pellet residue of these samples as analyzed by py-MBMS. This result suggests that, compared with cellulase enzymatic treatment, Fenton reaction is an aggressive treatment to break down the lignocellulosic matrix and liberate low molecular weight cellulosic carbohydrates. Sample 8's positive displacement territory along PC2 can be attributed to its relatively higher content of methoxylated lignin fragments (e.g., *m*/*z* 77, 124, 137, 150, and 272), as well as furan structures derived from altered carbohydrates (*m*/*z* 68). Compared with the significant difference in carbohydrate content, the changes in the structure of lignin were more subtle in these samples.

Brown-rot fungi are characterized by their ability to cause rapid strength losses early in the degradation process, which has been attributed to nonenzymatic mechanisms involving free radicals generated by the Fenton reaction. The results presented in this work confirm that iron-reducing CMFRs can effectively liberate cellulosic components from the wood substrate, allowing these components to be more accessible to further biodegradation by enzymatic or nonenzymatic means.

^{13}C-TMAH assessment of lignin oxidation

Figures 5 and 6 show the partial gas chromatograms of lignin monomers released after ^{13}C-TMAH thermochemolysis of wood residues and supernatants, respectively. The

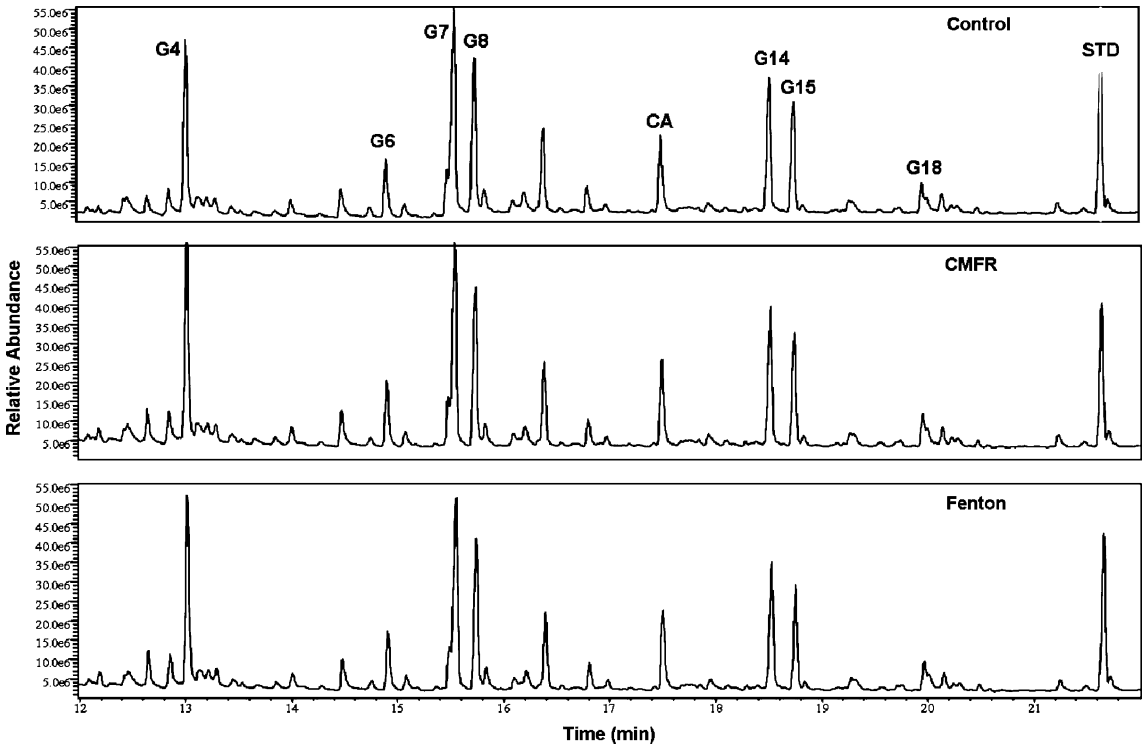

Fig. 5 Partial gas chromatogram of spruce wood residue before (control) and after treatment with Fenton reaction and chelator-mediated Fenton reaction (*CMFR*)

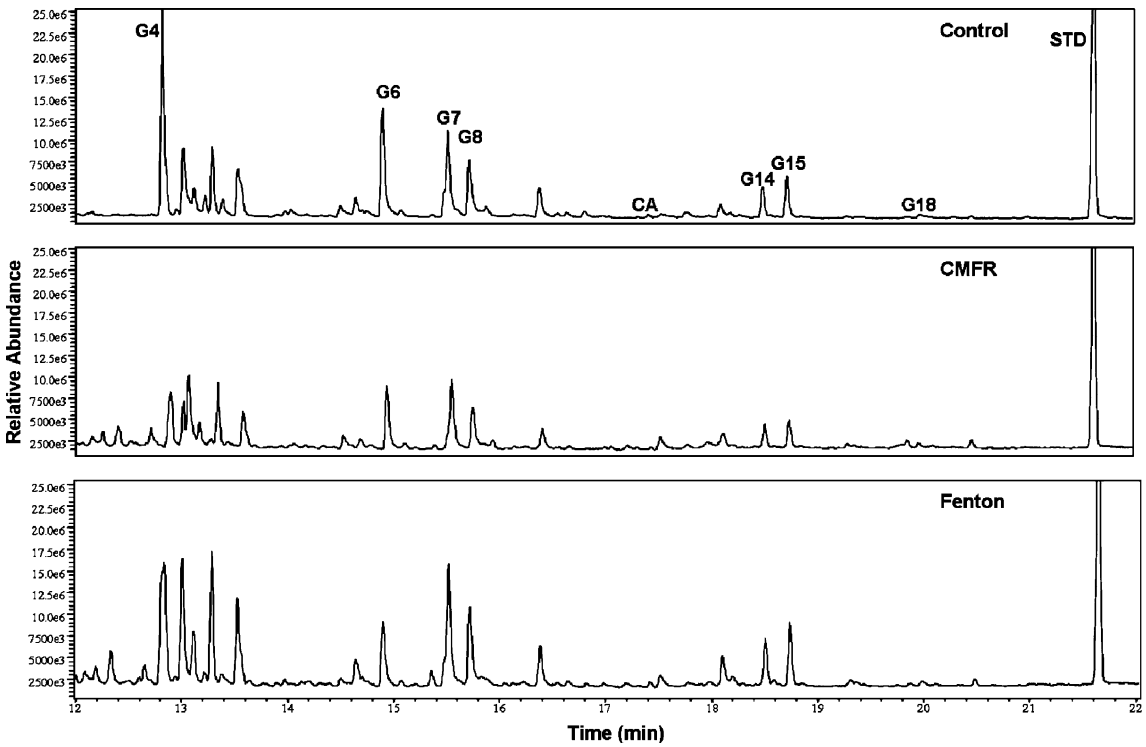

Fig. 6 Partial gas chromatogram of supernatant after spruce wood before (control) and after treatment with Fenton reaction and CMFR

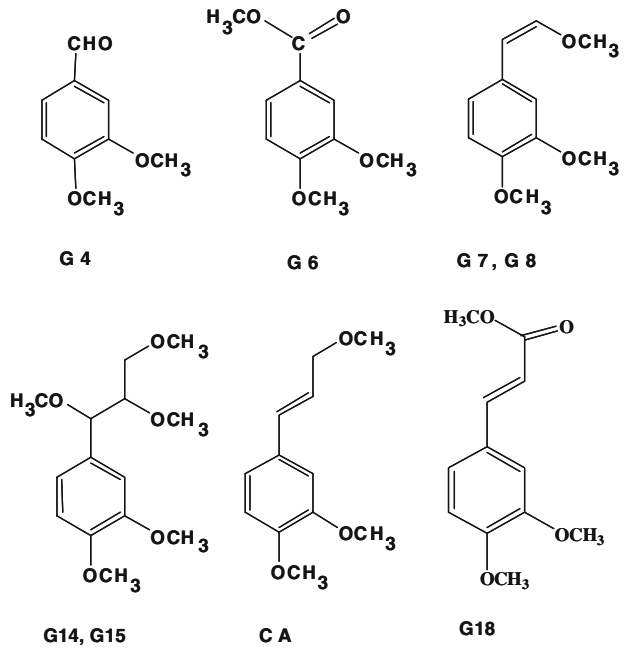

Fig. 7 Main products (permethylated structures) released from lignin after tetramethylammonium hydroxide thermochemolysis of softwood. *G4* 3,4-dimethyoxybenzaldehyde, *G6* 3,4-dimethoxybenzoic acid, methyl ester, *G7 cis*-1-(3,4-dimethyoxyphenyl)-2-methoxyethylene, *G8 trans*-1-(3,4-dimethyoxyphenyl)-2-methoxyethylene, *G14 threo*-1-(3,4-dimethoxyphenyl)-1,2,3-trimethoxypropane, *G15 erythro*-1-(3,4-dimethoxyphenyl)-1,2,3-trimethoxypropane, *CA* coniferyl alcohol, *G18* ferulic/caffeic acid

chemical structures and abbreviations of the eight major lignin monomers are listed in Fig. 7. The monomers identified are characteristic for a coniferyl-based gymnosperm lignin [8, 36, 37].

Comparison of the chromatograms indicates that the overall distribution of monomers in the untreated wood residue remains similar to that in the respective treated sample (Fig. 5). The dominant monomers in both samples included 3,4-dimethoxybenzaldehyde (G4), two isomers of 1-(3,4-dimethoxyphenyl)-2-methoxyethylene (G7 and G8), and two diastereomers of 1-(3,4-dimethoxyphenyl)-1,2,3-trimethoxypropane (G14 and G15).

When the supernatants of the treated and untreated wood samples were analyzed, some differences in the overall monomer distribution were seen (Fig. 6). The dominant compounds in the untreated supernatant were G4, 3,4-dimethoxybenzoic acid, methyl ester (G6), and the two isomers G7 and G8. The relative abundance of G4 in the treated supernatant samples decreased compared with that in untreated supernatant, but all of the other major compounds in the treated supernatants (G6, G7, and G8) increased. In TMAH thermochemolysis of guaiacyl lignin, G4 has been proposed to result from those β-O-4 linkages that contain adjacent hydroxyl groups on the propyl side chain [32]. Thus, the decrease in the relative yield of G4 in the supernatant sample may indicate that CMFR caused alteration of the β-O-4 linkages.

Table 3 Concentration of 3,4-dimethoxybenzoic acid, methyl ester (*G6*) (ng/µg sample) and G6 to 3,4-dimethyoxybenzaldehyde (*G4*) ratio

	G6	G6/G4
Wood residue		
Control	2.86 (±0.078)	0.33 (±0.041)
Fenton	2.79 (±0.066)	0.32 (±0.052)
CMFR	2.78 (±0.081)	0.31 (±0.065)
Wood supernatant		
Control	1.68 (±0.127)	1.66 (±0.030)
Fenton	0.64 (±0.091)	0.63 (±0.092)
CMFR	0.82 (±0.051)	1.24 (±0.151)

The ratio of G6 to G4 (acid/aldehyde) has been employed as an indicator of the relative state of degradation of lignin, with an increased ratio suggesting a higher degree of degradation. Unexpectedly the G6 to G4 ratio of the supernatant increased upon Fenton and CMFR treatments, likely owing to the decrease in yield of G6 (Table 3), whereas no significant difference was found between untreated and treated wood residues (Table 3). The decrease in the yield of G6 may be due to the presence of the iron in the supernatant used during treatment that might have stayed in the aqueous phase after centrifugation of samples.

Lignin demethoxylation

The lignin monomers released after reaction of wood residues and supernatants with ^{13}C-TMAH were assessed for their extent of demethoxylation, or increase in hydroxyl content, by calculating the level of ^{13}C methyl addition at position 3 on the aromatic ring. Any increase in the percentage of ^{13}C with respect to the untreated sample (control) is presumed to be the result of demethylation.

Figures 8 and 9 show the percentage of demethoxylation values for each of the lignin monomers from wood residue and supernatant samples, respectively. All of the monomers generated after ^{13}C-TMAH thermochemolysis of the wood residue exhibit only minor changes in the hydroxyl content relative to the untreated control sample (Fig. 8). Upon CMFR treatment, coniferyl alcohol (CA) displayed the highest increase in the hydroxyl content (1.7%), followed by G14 (0.3%) and G15 (0.4%) with minor increases, whereas G6, G7, G8, and ferulic/caffeic acid (G18) showed a decrease in the hydroxyl content relative to the untreated sample. Upon Fenton treatment, G6 and G18 were demethoxylated to about 2 and 3%, respectively, whereas G4, G8, CA, and G14 displayed a decrease in the

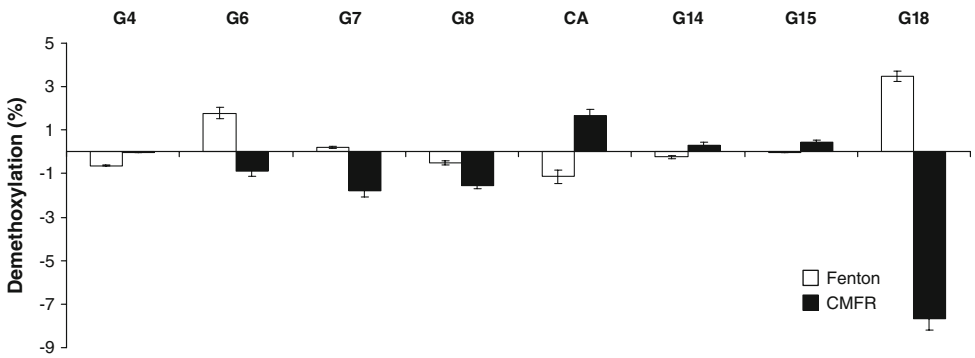

Fig. 8 Lignin demethoxylation of residue after wood treatment with Fenton reaction and CMFR

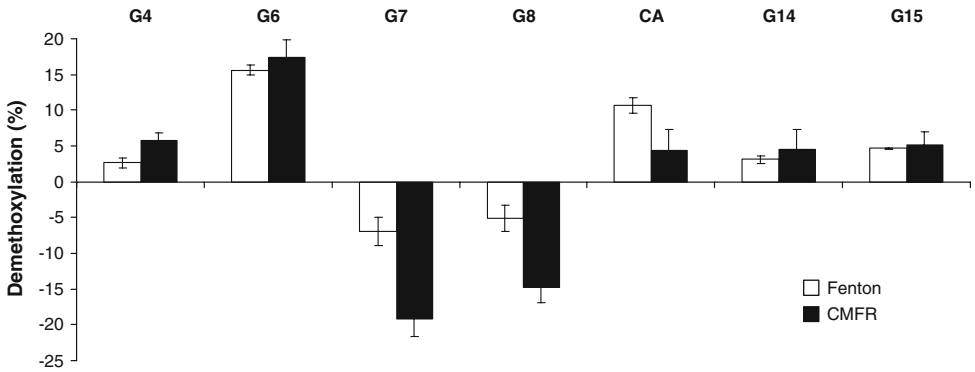

Fig. 9 Lignin demethoxylation of supernatant after wood treatment with Fenton reaction and CMFR

hydroxyl content relative to the untreated sample. The Fenton and CMFR treatment led to quite different demethoxylation profiles in wood residue samples, though the extent of the demethoxylation after both treatments was very limited in comparison with the control sample.

In contrast to the wood residue samples, the lignin monomers identified in the treated supernatants all exhibited a large alteration of hydroxyl content relative to the untreated control sample (Fig. 9). With the exception of G7 and G8, all monomers from Fenton- and CMFR-treated supernatant samples had greater hydroxyl content than the monomers from the control sample supernatant. This indicates that a considerable amount of demethoxylation occurred after Fenton and CMFR treatment and the monomers remained soluble and did not repolymerize extensively. The highest degree of Fenton and CMFR demethoxylation, at 15.6 and 17.4%, respectively, was found for G6 released from the wood residue and identified in the treated supernatants.

The wood residue obtained after ground wood treatment with CMFR and with Fenton reaction exhibited only minor changes in percentage of demethoxylation with respect to the untreated sample material (Fig. 8). On the other hand, most monomers, excluding G7 and G8, from supernatants showed significant increases in their percentage of aromatic hydroxyl, especially for G6 (Fig. 9), indicating that demethoxylation of the 3-methoxyl carbon has occurred during CMFR and Fenton treatments, generating 3,4-dihydroxyphenyl structures in the lignin. Unlike the wood residue monomers, the overall change in the hydroxyl content of supernatant monomers was very similar for Fenton reaction and CMFR. In general, the CMFR treatment produced greater demethoxylation, especially for G7 and G8.

In brown-rotted wood residues, demethoxylated lignin is abundant [9, 22]. The lack of demethoxylated monomers in the wood residue in the current study was therefore difficult to explain until analysis showed the demethoxylated fragments in the supernatant. In brown-rotted wood, there is no fluid flow that would permit extensive extraction of the soluble demethoxylated monomers out of the wood, and continued oxidation via free radicals likely results in the bulk of the monomers repolymerizing with other residual lignin fragments. In a natural decay environment, some fragments are likely to be soluble for some time and may function to bind and reduce iron, as has been previously proposed for participation in CMFRs [20, 21]. Laboratory simulations of natural systems are unable to capture all of the parameters of the natural model perfectly. The current research provides a close, but not perfect, model of the fungal-wood environment. Mixing the wood and reactants in a buffered medium solution simulates the natural decay environment, but provides greater opportunity for soluble fragments to diffuse from the lignin to be recovered in the supernatant fraction.

The decrease in hydroxyl content of G7 and G8 from treated supernatants may be an indication of further degradation or selective polymerization of the *ortho*-hydroxy

functionality. Similarly, Filley et al. [38] also found that some of the monomers released after ^{13}C-TMAH thermochemolysis of the brown-rot-decay wood residue had lower hydroxyl content than fresh wood. In this context, Harvey et al. [39] (as reported in [40]) proposed that brown-rot fungi repolymerize lignin because highly unstable radical cation intermediates formed from phenolic-containing aromatic compounds are oxidized by a single electron. These phenoxy radicals undergo further reactions, including oxidative carbon-to-carbon and carbon-to-oxygen coupling reactions, to produce higher molecular weight products that the brown-rot fungi evidently cannot metabolize.

It has been demonstrated that lignin in wood subjected to brown-rot decay, in addition to undergoing extensive demethoxylation, also undergoes some side chain oxidation [8, 20] and our results indicate that Fenton-based reactions are also capable of promoting lignin side chain oxidation. In this regard, the monomer G4 is proposed to result from the TMAH thermochemolysis of β-O-4 linkages that contain adjacent hydroxyl groups on the propyl side chain [32]. Thus, the relative abundance of G4 may be indicative of the degree of alteration of those β-O-4 linkages [32]. It follows therefore that a significant decrease of the relative intensity of G4 in the treated supernatant compared with the untreated supernatant (Fig. 6) is indicative of the loss of lignin structures containing β-O-4 aryl ether hydroxy subunits upon CMFR and Fenton treatments. Further, in the lignin supernatant samples, the percentage of demethylation of the oxidized monomer G6 is greater than the percentage of demethylation of the G14 and G15 monomers (Fig. 9). G6 obtained after TMAH thermochemolysis of undegraded and degraded wood could be derived from the methylation of free vanillic acid, cleavage of an ether-bound vanillic acid residue, cleavage of a lignin subunit in an intermediate oxidation state, or, as shown previously [38, 41], as a reaction by-product from untreated lignin. G14 and G15 contain the fully methylated glycerol side chain and their structures are near to the structure of the complete methylated lignin monomer. These compounds are also thought to be indicative of undegraded β-O-4 linkages with adjacent hydroxyl groups in the sample [32, 41]. Their presence in the TMAH thermochemolysis products of natural lignin-containing samples indicates that some portion of the sample contains lignin fragments that have not undergone complete side chain oxidation. Therefore, greater percentages of G6 demethylation than G14 and G15 demethylation may indicate that vanillic acid structures are generated prior to demethylation of the methoxyl carbon, suggesting that some side chain oxidation occurs prior to demethylation.

Conclusions

It is well documented that during brown-rot wood decay, the lignin structure is modified mainly through demethylation, generating a residue enhanced in hydroxyl content. However, although reactive oxygen species generated through Fenton-based reactions have been suggested to be the causative agent of lignin modification, there has been no direct evidence showing that the reactions can actually occur under conditions simulating brown-rot wood decay. The results presented herein demonstrate that Fenton-based reactions are capable of causing demethoxylation of lignin in wood. It should be noted, however, that in natural oxygenated environments, ferric iron predominates and little ferrous iron will be found. Therefore, brown-rot fungi produce iron chelators, at least one mechanism to reduce iron in nature and to permit the production of ferrous iron in specific locations of the wood cell wall. This in turn promotes the CMFR and the depolymerization of the cell wall components. In the brown-rot fungi studied, this system appears to be the predominant method for reducing iron and initiating fungal degradation of wood.

Acknowledgments We appreciate the support of the Department of Earth and Atmospheric Sciences at Purdue University for the ^{13}C-TMAH thermochemolysis work, the Wood Utilization Research Center at the University of Maine for the financial support for the collaborative research conducted at Purdue University, and support from the National Renewable Energy Laboratory in Golden, Colorado, for their MBMS facilities and support staff. V.A. is also grateful to the Coordination for the Improvement of Higher Level Personnel (CAPES-Brazil) Grant No. 5192/06-4 for the financial support for his stay at the Wood Science and Technology Laboratories at the University of Maine, Orono, Maine, USA. This is paper 3058 of the Maine Agricultural and Forest Experiment Station.

References

1. Bagley ST, Richter DL (2002) The mycota. In: Osiewacz HD (ed) Industrial applications, vol 10. Springer, Berlin, pp 327–341
2. Goodell B (2003) In: Goodell B, Nicholas D, Schultz T (eds) Wood deterioration and preservation: advances in our changing world. American Chemical Society Series. Oxford University Press, New York, pp 97–118
3. Cowling EB (1961) Technical bulletin 1258. US Department of Agriculture, Washington, p 79
4. Kirk TK, Highley TL (1973) Phytopathology 63:1338–1342
5. Agosin E, Jarpa S, Rojas E, Espejo E (1989) Enzyme Microb Technol 11:511–517
6. Ander P, Stoytschev I, Eriksson K-E (1988) Cellul Chem Technol 22:255–266
7. Enoki A, Tanaka H, Fuse G (1988) Holzforschung 42:85–93
8. Filley TR, Hatcher PG, Shortle W (2000) Org Geochem 31:181–198
9. Jin L, Schultz TP, Nichols DD (1990) Holzforschung 44:133–138
10. Niemenmaa O, Uusi-Rauva A, Hatakka A (2008) Biodegradation 19:555–565
11. Goodell B, Jellison J, Liu J, Daniel G, Paszczynski A, Fekete F, Krishnamurthy S, Jun L, Xu G (1997) J Biotechnol 53:133–162
12. Arantes V, Milagres AMF (2009) Quim Nova (in press)

13. Arantes V, Milagres AMF (2006) J Chem Technol Biotechnol 81:413–419
14. Enoki A, Itakura S, Tanaka H (1997) J Biotechnol 53:265–272
15. Kerem Z, Jensen KA, Hammel KE (1999) FEBS Lett 446:790–797
16. Paszczynski A, Crawford R, Funk D, Goodell B (1999) Appl Environ Microbiol 65:674–679
17. Arantes V, Milagres AMF (2006) J Hazard Mater 141:273–279
18. Arantes V, Baldocchi C, Milagres AMF (2006) Chemosphere 63:1764–1772
19. Contreras D, Rodríguez J, Freer J, Schwederski B, Kaim W (2007) J Biol Inorg Chem 12:1055–1061
20. Filley TR, Cody GD, Goodell B, Jellison J, Noser C, Ostrofsky A (2002) Org Geochem 33:111–124
21. Xu G, Goodell B (2001) J Biotechnol 87:43–57
22. Jin L, Nicholas DD, Kirk TK (1990) Wood Sci Technol 24:263–276
23. Gierer J, Yang E, Reitberger T (1992) Holzforschung 46:495–504
24. Gierer J (1997) Holzforschung 51:34–46
25. Lanzalunga O, Bietti M (2000) J Photoch Photobio B 56:85–108
26. Machado AEH, Furuyama AM, Falone SZ, Ruggiero R, Perez DDS, Castellan A (2000) Chemosphere 40:115–124
27. Kelley SS, Jellison J, Goodell B (2002) FEMS Microbiol Lett 209:107–111
28. Kelley SS, Rowell RM, Davis M, Jurich C, Ibach R (2004) Biomass Bioenerg 27:77–88
29. Evans RJ, Milne TA (1987) Energ Fuel 1:123–137
30. Martens H, Naes T (1991) Multivariate calibration. Wiley, New York, 419 pp
31. Wold S, Ebensen K, Geladi P (1987) Chemometr Intelligent Lab Syst 2:37–52
32. Filley TR, Minard RD, Hatcher PG (1999) Org Geochem 30:607–621
33. Barr DP, Aust SD (1994) Environ Sci Technol 28:78–87
34. Wayman M, Chua MGS (1979) Can J Chem 57:2612–2616
35. Yelle D, Raph J, Lu F, Hammer KE (2008) Environ Microbiol 10:1844–1849
36. Challinor JM (1995) J Anal Appl Pyrol 35:93–107
37. Hatcher PG, Nanny MA, Minard RD, Dible SD, Carson DM (1995) Org Geochem 23:881–888
38. Filley TR, Nierop KGJ, Wang Y (2006) Org Geochem 37:711–727
39. Harvey PJ, Schoemaker HE, Palmer JM (1986) Document IRG/WP/1310, International Research Group on Wood Preservation
40. Highley TL, Dashek WV (1998) In: Bruce A, Palfreyman JW (eds) Forest products biotechnology. Taylor & Francis, London, pp 15–36
41. Hatcher PG, Minard RD (1995) Org Geochem 23:991–994